Blown film thickness control with a scanning down-the-line measurement

Mikko Salo and Risto Ritala

Abstract— **The thickness profile of the tubular bubble in blown film extrusion is deduced from delayed measurements made downstream in the flatted web consisting of the bubble. Scanner moving across the web measures only a portion of it at a time and the measurement results are matched to the bubble profile at actuators controlling the thickness. The delayed profile is predicted to current time and used for LQR feedback control. The control architecture is tested in a simulation of the process.**

I. INTRODUCTION

In the blown plastic film extrusion process, there are generally two ways to measure the thickness of the plastic film [1]. Direct, one-sided measurements around the circumference of the blown bubble yield the manipulable outputs directly with little transport delay. The geometry of the process makes these measurements limited in practice however and contact with the plastic film and frequent calibrations are often required [2]. An alternative way is to measure the flattened two-layer web before reeling from both sides. This method may open options for more accurate and practical measurement systems such as radiation absorption [3] or distance measurements [4], but more intricate estimation methods are required. The measurement of the web consists of two-layer thick plastic and the profile of the bubble that it is made of by flattening is needed for control. Delays from the actuators to the web are also longer than to the bubble. The proposed method is not tested against existing control architectures in the scope of this paper.

One-sided measurements consist of a sensor moving around the bubble. Some proposed and used methods in the past include capacitive sensing [5], laser triangulation [6], low-coherency interferometry [2] and optical coherence tomography [7].

This paper proposes a measurement, estimation and feedback control architecture for the blown plastic film extrusion process using data obtained from the flatted web. The problem of how to deduce the thickness profile of a tubular structure from data of its flattened two-layer thickness is studied. The problem becomes even more complicated, since different measurements across the width of the material are made at different time instances due to the motion of the scanner. The transportation delays of the material also change with time. The measurement data is obtained by a moving scanner and the thickness of the plastic along the circumference of the bubble at the actuators is deduced and used for control in a simulation environment.

The process of blown film extrusion is introduced more in detail in Section II. Section III derives the architecture for deducing the tubular thickness as well as ties it to known control methods, forming a closed-loop control architecture for the thickness of the film. A simulator of the process has been built in Matlab and it is introduced in Section IV. A simulation case of the control architecture is also shown. The results of the simulation case are discussed in Section V.

II. BLOWN FILM EXTRUSION

Molten plastic polymer is fed along a circular die ring with a diameter of around 0.45m by extruders through a controllable slice opening. Air is blown around or through the middle of the die ring, causing the plastic to form a vertically traversing (either upwards or downwards depending on the process) bubble of up to 15 meters tall that cools and solidifies along the way, as well as expands . The diameter of the expanded solid bubble varies between 0.7m-1m depending on process conditions. Water is sometimes used outside the bubble to cool the plastic faster. The height of the molten plastic is called the frost layer height and the speed of the plastic bubble in machine direction (MD) after solidifying is called nip speed. The solid bubble moves through a combination of a collapsing frame and nip rollers, hereby referred to as flatter, that flatten it. The collapsing frame guides the plastic and becomes more narrow, until reaching the nip rollers that finally squeeze the plastic bubble resulting in a two-layer flat web of width 1m-1.5m. The flattened web travels through a multitude of idle rollers in different angles to align the web depending on process geometry. The web travels in MD at speeds of 15-50 meters per minute and is reeled to a shippable product. The web thickness is locally measured in cross-direction (CD, the circumference of the bubble) by a scanner moving back and forth.

The flatter rotates along its axis to prevent possible variations in the thickness of the film in CD from building up in one section of the reeled web. This back and forth rotation causes a twist in the bubble material between the die ring and the flatter. In the use case of this paper, the flatter rotates between 0-350 degrees at a rate of 350 degrees per 15 minutes of time. Due to the geometry of the process and rotation of the flatter, the distance from the flatter to reeling (and scanning) also changes as a function of the flatter angle as much as 11m between end positions. The web tension in MD is kept constant by changing the rate of the reeling according to the flatter motion.

[1]Mikko Salo is with the Faculty of Engineering and Natural Sciences, Tampere University, Tampere, Finland mikko.salo@tuni.fi

[2]Risto Ritala is with the Faculty of Engineering and Natural Sciences, Tampere University, Tampere, Finland risto.ritala@tuni.fi

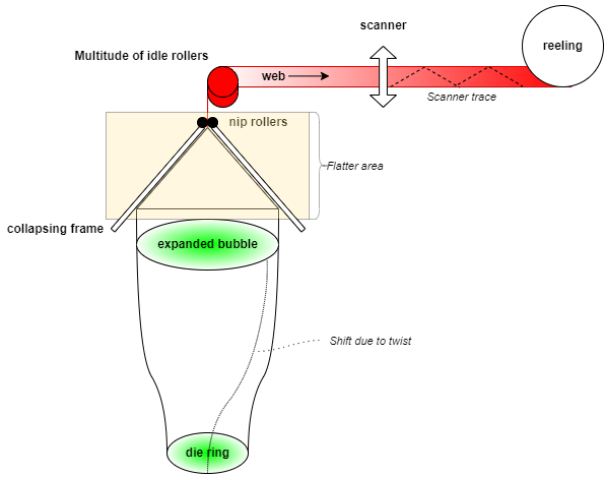

Fig. 1. A diagram of the process

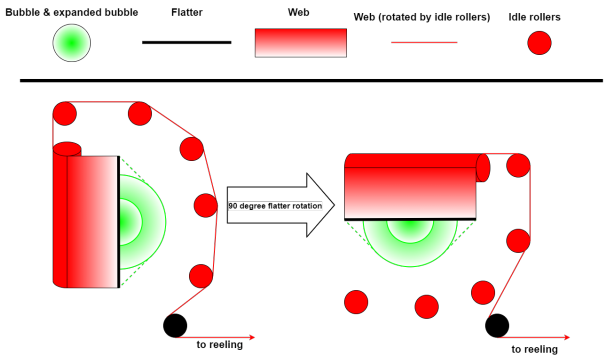

Fig. 2. Process diagram along the longitudinal axis of the bubble with two different flatter angles

A scanner measures the thickness of the two-layer plastic web between the flatter and reeling using beta radiation absorption. The scanner measures only a portion of the web at any given time instance and moves across the web in CD back and forth at a rate of approximately 14 seconds per pass. Whenever the scanner reaches the edge of the web, a CD profile of the data obtained is created and stored and the scanner changes direction after a brief period of cleaning etc. A diagram of the process from die ring to reeling can be seen in Figure 1.

The thickness of the plastic film is controlled using 48 slice opening actuators spaced out evenly across the die ring. Opening the slice causes more mass flow centralized around the actuator, increasing the film thickness in that part of the CD. Other factors that affect the thickness are for example extruder melt quality and expanded bubble diameter. These are assumed to be kept constant in the simulations of this study.

The values and process geometry given are those of a specific real plant. The blown film extruder process can vary a lot depending on the plant and has a multitude of different control and measurement options. Frost layer height, bubble size and extruder melt quality are among the common controllable variables. A more detailed and general analysis of the entire process can be found for example in [1] and [8].

III. CONTROL ARCHITECTURE

A. Delays

The delay from the die ring to the flatter is constant d_0, but the delay from flatter to scanner varies as a function of the flatter angle. The length $L(t)$ of the web from flatter to scanner as well as the rate of change

$$\frac{dL(t)}{dt} \tag{1}$$

in the length of the web is assumed known for each time instant t from process geometry and the flatter angle and angular velocity. Figure 2 shows the change in the length of the web.

The velocity of the web before the flatter is constant v_0. At time T_2 a scanner measurement is made. Let T_1 be the time instant the corresponding MD segment of the web passed the flatter. Then $d = T_2 - T_1$ is the desired delay. If the web tension is to be kept constant, the reeling rate must change in a way that compensates for the change in the length of the web. The velocity the MD segments experience after the flatter due to change in reeling rate is then

$$v_r\left(t\right) = -\frac{dL\left(t\right)}{dt}. \tag{2}$$

In an infinitesimal time dt, the MD segment in question travels a distance

$$\left(v_0 + v_r(t)\right) dt. \tag{3}$$

Since the distance from flatter to scanner for the MD segment does not change after it has left the flatter, it holds that

$$\begin{aligned} L\left(T_1\right) - \int_{T_1}^{T_2} v_0 - \frac{dL\left(t\right)}{dt} dt = 0 \\ \implies d_{T_2} = \frac{L\left(T_2\right)}{v_0}. \end{aligned} \tag{4}$$

B. State space model

The process is modeled as a zero-order hold integrative discrete time state space [9]

$$x_{n+1} = x_n + Bu_n + \epsilon_n, \quad \epsilon_n \sim N(0, \Sigma^{(p)}), \tag{5}$$

where x_n are state[1] vectors, u_n the vectors of control actions and ϵ_n is Gaussian white noise for each discrete time instant n. Matrix B is the control dynamics matrix and defines how the control action u_n affects the states. The circumference of the die ring is divided into even number X equal sized databoxes. The plastic film thicknesses in each databox is assumed uniform and a discrete state space model (5) is

[1]The states are referred to as real states (as opposed to estimated) in the future even though they are simulated in this case

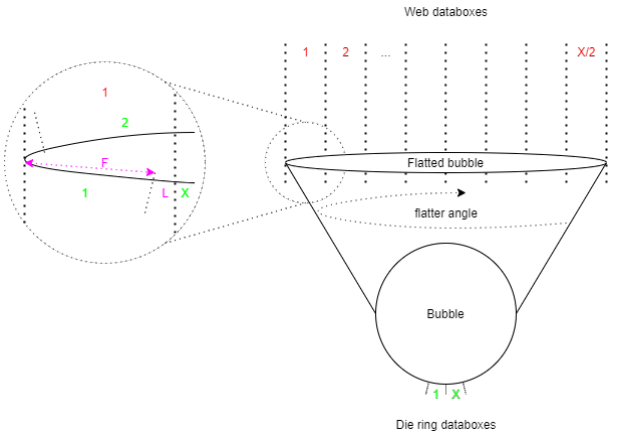

Fig. 3. Web databox interpolation. Red numbers refer to web indices and green to die ring indices.

formed with the thicknesses in each databox representing the state vector $x_n[J]$[2], $J = \{1, \ldots, X\}$.

The plastic film web at the flatter is divided into $\frac{X}{2}$ databoxes. The web left edge x_L is defined as the position of the left edge of the web in continuous die ring coordinates and is formed from the flatter angle. The web thickness profile at the flatter $f_n[I]$, $I = \{1, \ldots, \frac{X}{2}\}$, is formed from the state x by summing and interpolating the opposing databoxes with respect to the flattening axis and delays. For all $i \in I$

$$\begin{aligned} \alpha f_n[i] = {} & F_n x_{n-d_0}[mod(L_n + i, X) + 1] \\ & + (1 - F_n) x_{n-d_0}[mod(L_n + i - 1, X) + 1] \\ & + F_n x_{n-d_0}[mod(L_n - i + 1, X) + 1] \\ & + (1 - F_n) x_{n-d_0}[mod(L_n - i, X) + 1], \end{aligned} \tag{6}$$

where α is the bubble diameter expansion factor from die ring to flatter,

$$\begin{aligned} L_n &= floor\left(mod\left(x_{L,n} - w_n,\ X\right)\right) \\ F_n &= mod\left(x_{L,n} - w_n,\ 1\right) \end{aligned} \tag{7}$$

and w_n is the index shift due to the twist. The interpolation is depicted visually in Figure 3.

The scanner measurements $s_n[I]$ are modeled by detecting the web databox values at the scanner current location i and adding a Gaussian white noise component:

$$s_n[i] = f_{n-d_n}[i] + \nu_n, \quad \nu_n \sim N(0, \Sigma^{(m)}), \tag{8}$$

where ν_n is the measurement noise with a covariance matrix $\Sigma^{(m)}$. The simulated measurement system in this study mimics an IQ Quality Control System (QCS). The QCS scanner is used for example in the basis weight control of a paper mill, where the measurement of the paper web is analogical to that of a flattened two-layer plastic sheet [10].

[2]Vector notation: sub-indices refer to discrete time instant, bracketed variables refer to element index or set of indices.

A total of N actuators are uniformly distributed along the ring and their response models in the states form the model $\hat{B}$ of the control dynamics matrix B. The matrix $\hat{B}$ is a model of the actuator effects, hence it may not be the same as the actual control effects matrix B in (5). The optimal steady state LQR-control law is

$$u_n = (\hat{B}^\intercal \hat{B})^{-1} \hat{B}^\intercal m_n, \tag{9}$$

where m_n is the difference of the current state vector and a given control goal. Generally, the state vector x_n is not known to a certainty, and an estimate is used to calculate the control action [11].

The optimal steady state control law, when applied to (5), yields a state that has minimum sum of squared error of state and control goal at the next time step, assuming that the actuator effects are instantaneous. In real-life processes however, the actuator effects on the state usually have a rise time and the optimal control law may not be applied fully at the risk of overshoot and even instability. Moreover, if measurements or estimation method of states are delayed or have dynamics, the control action (9) must also be throttled [12].

C. Deducing past state from measurement data

The states can be deduced when delays, flatter positions and twists are known. Assume scanner has obtained a measurement result $s[i]$ at web databox i at a time instant $n = n(i)$. Define

$$\begin{aligned} L^{(d)}[i] &= floor(mod(x_{L,n-d_n} - w_{n-d_n}, X))) \\ F^{(d)}[i] &= mod(x_{L,n-d_n} - w_{n-d_n}, 1), \end{aligned} \tag{10}$$

Then it holds that

$$\begin{aligned} & F^{(d)}[i] x[mod(L^{(d)}[i] + i, X) + 1] \\ & + (1 - F^{(d)})[i] x[mod(L^{(d)}[i] + i - 1, X) + 1] \\ & + F^{(d)}[i] x[mod(L^{(d)}[i] - i + 1, X) + 1] \\ & + (1 - F^{(d)})[i] x[mod(L^{(d)}[i] - i, X) + 1] = s[i]. \end{aligned} \tag{11}$$

Equation (11) shows how the measured web databox has formed from the two opposed sides of the flattened bubble with delays and interpolation between consequent databoxes since the web left edge is continuous.

Due to the motion of the scanner across the web, the time instance n in (10) is a function of the measured web databox index i. Hence for each scanner pass over the entire web there exists $\frac{X}{2}$ equations like (11), forming a system of equations

$$Ax = s. \tag{12}$$

The elements of the matrix A are the interpolation factors. The corresponding indices of the elements of A are given by the indices of x in (11) for each row respectively. The state vector x has X elements, so a bare minimum of two scanner passes is required to reasonably solve the state vector.

A least squares solution for the system of equations is given by the Moore-Penrose pseudoinverse defined as [13]

$$A^{+} = \lim_{\delta \to 0} \left(A^{\intercal} A + \delta Id\right)^{-1} A^{\intercal}, \tag{13}$$

where Id is an identity matrix the size of $A^{\intercal}A$. For practical computations, the pseudoinverse can be approximated with a small δ. The pseudoinverse is unique and it holds that

$$\hat{x}_n^{(d)} = \alpha A^{+} s \tag{14}$$

is a least squares solution for (12). The factor α is taken into account since the system of equations (12) realizes the reduced thickness of the film, but not the increased size of the databox, that are caused by the expanding bubble. The solution $\hat{x}_n^{(d)}$ is called the deduced state where n refers to the time of deduction, which is the time instance when the scanner has passed over the entire web. This is also the control interval.

Note that the solution to the system of equations does not represent the state vector x at any single time instance since the measurement data s is obtained over several time instances and the delays are also varying.

Other least squares solutions exist that differ in this case (for example Matlab mldivive), but simulation environment has shown that the Moore-Penrose pseudoinverse gives a more sensible solution to match the real state of the process.

D. Prediction

Even though the deduced past state is not tied to any specific time instant, it is delayed and represents the state somewhere between the time instances when the first and last measured databox values used in the deduction were created at the actuators. The control actions affect the state x much sooner than they are detected in the deduced state $\hat{x}^{(d)}$, hence prediction is necessary. The formula for predicting the current state x_n from the deduced state $\hat{x}_n^{(d)}$ and control actions u is [10]

$$\hat{x}_n = \hat{x}_n^{(d)} + \hat{B}(u_n - u_{n-T_n}), \tag{15}$$

where T_n is the delay used to describe the deduced past state and $\hat{x}_n$ is the estimate of the current real state x_n. The delay T_n depends on the varying transport delay from the actuators to the scanner, as well as the number of scanner profiles used to deduce the state $\hat{x}_n^{(d)}$. The choice of delay T_n will cause temporary over- or undershoot between the predicted state $\hat{x}_n$ and the real state x_n when control actions are detected by the scanner profiles.

E. Control

The control action is calculated and applied whenever the deduction and prediction are done, namely when the scanner reaches the edge of the web and a profile is created. The control action is calculated according to (9) where $m_n = x_n - \hat{x}_n$ is the difference of the real state and the estimate at the current time step n. Since the measurement is delayed and the deduction is done from data of multiple time instances, the control action must be throttled. A factor

$$\delta_n = \frac{1}{C_n} \tag{16}$$

is given to the calculated control action, where C_n is the current transport delay in control intervals plus a the amount of scanner profiles used in deducing the past state $\hat{x}_n^{(d)}$. This is the amount of control intervals in which all the scanner profiles used in deduction have detected the actuator effects.

F. Identifying bubble twist

The twist can be approximated from plant or simulator data by creating estimates in both flatter directions without accounting for twist and comparing them. Since the twist is in the direction of the flatter rotation, the different estimates will show a shift into opposite directions. Comparing the data by cross-correlation, the twist can be approximated given that the state does not change significantly between estimates. The steps for identifying the twist are:

- Generate estimates when flatter is rotating in both directions.
- Take average of estimates for each direction
- Compare averages using cross-correlation
- The displacement that yields the highest correlation corresponds to approximately two times the twist
- Interpolation may be used to find a continuous, more accurate twist.

The twist can be identified for example in the start-up period of the process, and a look-up table for twists for different materials may be created.

IV. Simulation studies

A. Simulator

A simulator of the blown film extrusion process has been built in Matlab. The simulation loops in time. At each unit time step n:

- The next real state x_n is generated from previous state x_{n-1}, control actions, external disturbances and process noise.
- The flatter angle is changed according to previous angle and angular velocity.
- Flatted web profile f_n is generated from flatter angle and past state x_{n-d_0} by interpolating and summing corresponding databoxes.
- Scanner is moved according to its parameters and scanner measurement data $s_n[I']$ is generated from past flatted web profile $f_{n-d_n}[I']$, where I' are the web indices the scanner passed. The measurement data is stored into an active CD profile in the databoxes the scanner passed.
- If scanner reached the end of the web, estimate and control action are calculated according to Sections III-C, III-D and III-E, and control is applied to next time step.

All parameters in the simulator are adjustable to describe a given scenario.

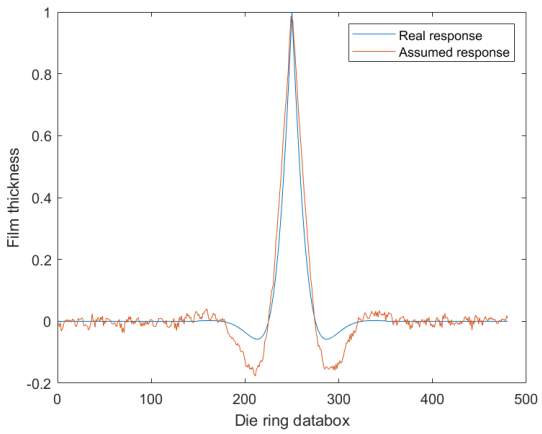

Fig. 4. Simulated (B) and estimated ($\hat{B}$) actuator steady state response models for a single actuator at the die ring

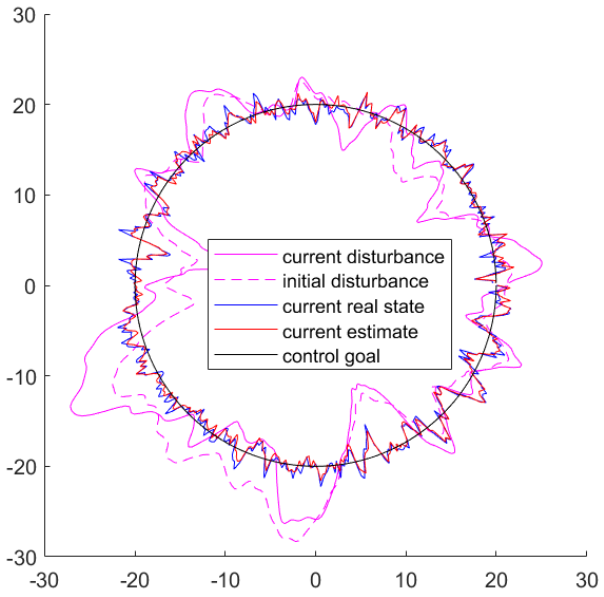

Fig. 5. Die ring profile in polar plot after load disturbance has settled

B. Control of dynamic unknown load disturbance

The ability of the estimation to detect and the control to correct load disturbances changing in time was tested. In the test scenario, the die ring profile is initialized randomly and another profile whose magnitude increases in time is added. Estimation and control are turned on once the simulator has generated enough data at the scanner location. This is to say, when the scanner has made at least 3 passes over the web, which is well under a minute given the 14 seconds scanner pass and pauses out of the web. Hence the startup of the control does not require any additional steps and it can be used when the process is started up.

The simulation also contains process noise as well as scanner measurement noise. The bubble twist is turned on, but assumed known. The actuator response model used in prediction and calculating the control differs from the actual model that generates the real states to emulate uncertainty in identifying it. The real and assumed models are depicted in Figure 4. The figure shows the actuator dynamics B used to generate the real state x as well as it's model $\hat{B}$ used to calculate the control law and in prediction. The model was generated in a step response test using simulator generated data and the estimation method.

The results of the simulation are depicted in Figure 5. Real state in the figure refers to the one generated by the simulator according to (5). Estimate is $\hat{x}$ as in (15). Initial disturbance is the value of the real state x in the beginning with zero control action. Current disturbance is the initial state plus the changing load disturbance at the current time.

V. Conclusions Discussion

The simulation test in IV-B shows promising results for the control architectures ability to detect and correct changing load disturbances as well as regulate the process. The scanner-based estimation method proposed replicates the real state very accurately when the states are not changing rapidly even when such obstacles as process and measurement noise, varying delays and bubble twist are added to the simulation. The residual between the control goal profile and the achieved state is not because of the control architecture, but due to lack of actuator capability and process noise [14].

Other simulations have been ran in a number of different scenarios, for example:

- How the number of scanner profiles affects the quality of the estimates and the estimation dynamics
- How fast a reliable estimate is obtained after a step change in the state
- How indexing errors, caused for example by misidentified twist affect the control efficiency

Some of the simulation parameters, such as process geometry and delays, are based on a real plant. Some parameters, like actuator response model, disturbances and control goal, were given made-up but realistic values to complete the simulations. Due to lack of comparable data, the control architecture introduced was not tested against other proposed or in-use control systems. The main benefit of the the proposed architecture would be the accuracy and reliability of the measurement system itself. The major downsides are the delays and inaccuracies due to matching the web and bubble indices.

As future work, other existing control architectures could be built into the simulator with comparable statistics to those of the proposed one and their outcomes could be compared. Effort is also taken to test the control architecture in a real plant.

ACKNOWLEDGMENT

This study was started in 2021 as a part of Business Finland APASSI project, and continued as a co-operation of Tampere University and Valmet Automation. A special thank you to Markku Mäntylä of Valmet Automation for coming up with the idea with Risto Ritala in the beginning of the

project and providing this opportunity. A thank you goes to Matti Vilkko of Tampere University as well for providing assistance in the finishing touches of this paper.

REFERENCES

[1] K. Cantor, Blown film extrusion, second edition. Edition, Hanser Publishers, Cincinnati, Ohio, 2011.

[2] M. Norgia, A. Pesatori, Interferometric instrument for thickness measurement on blown films, Photonics 8 (7) (2021) 245–.

[3] K. Leiviskä, Papermaking science and technology. Book 14, Process and maintenance management, 2nd Edition, Paper Engineers' Association, Helsinki, 2009.

[4] A. Piegari, E. Masetti, Thin film thickness measurement: A comparison of various techniques, Thin Solid Films 124 (3) (1985) 249–257. doi:https://doi.org/10.1016/0040-6090(85)90273-1.

[5] C. Loughlin, Sensors for industrial inspection (1993).

[6] J. P. Peterson, R. B. Peterson, Laser triangulation for liquid film thickness measurements through multiple interfaces, Applied optics (2004) 45 (20) (2006) 4916–4926.

[7] W. Drexler, J. G. Fujimoto, Optical coherence tomography : technology and applications, Biological and medical physics, biomedical engineering, Springer, Berlin, 2008.

[8] B. A. Morris, The science and technology of flexible packaging : multilayer films from resin and process to end use, Plastics design library, Elsevier, Boston, MA, 2017 - 2017.

[9] J. B. Burl, Linear optimal control : H2 and H[infinity] methods, Addison-Wesley, Menlo Park (CA), 1999.

[10] J.-P. Raunio, R. Ritala, Active scanner control on paper machines, Journal of Process Control 72 (2018) 74–90. doi:https://doi.org/10.1016/j.jprocont.2018.09.012.

[11] G. Franklin, J. Powell, M. Workman, Digital Control of Dynamic Systems-Third Edition, Addison-Wesley, 2006.

[12] H. Zhang, Control and estimation of systems with input/output delays, 1st Edition, Lecture Notes in Control and Information Sciences, 355, Springer, Berlin, Germany ;, 2007.

[13] A. E. Albert, Regression and the Moore-Penrose pseudoinverse, Mathematics in science and engineering ; v. 94, Academic Press, New York, 1972.

[14] D. P. Bertsekas, Dynamic programming and stochastic control, Mathematics in science and engineering ; v. 125, Academic Press, New York, 1976.